

SUPPLEMENTAL MATERIAL

for the manuscript by

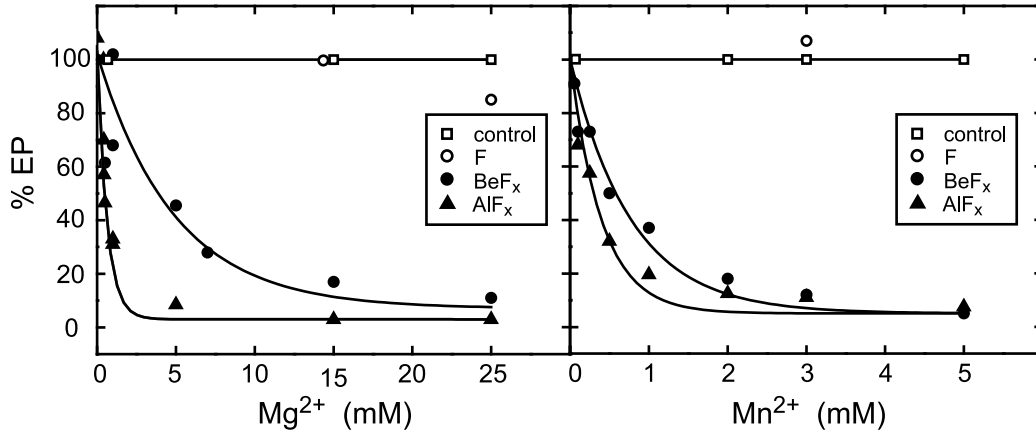
Stefania Danko, Takashi Daiho, Kazuo Yamasaki, Xiaoyu Liu, and Hiroshi Suzuki

**Formation of Stable Structural Analog of ADP-sensitive Phosphoenzyme
of Ca²⁺-ATPase with Occluded Ca²⁺ by Beryllium Fluoride**

STRUCTURAL CHANGES DURING PHOSPHORYLATION AND ISOMERIZATION

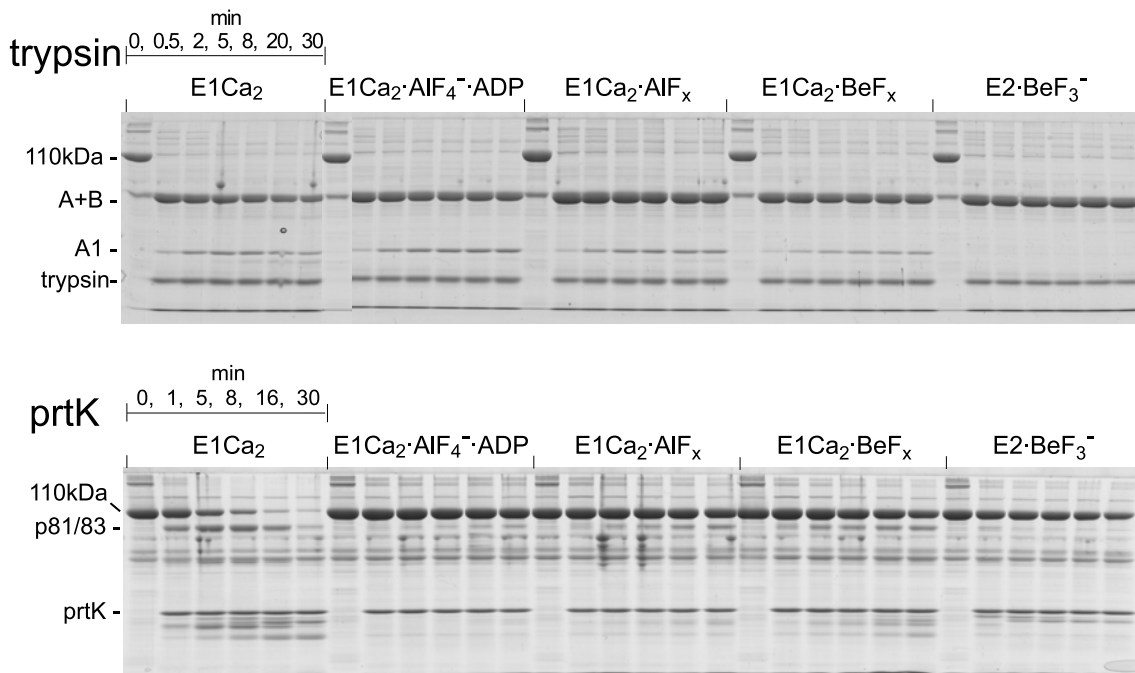
Supplemental Figure 1.

Mg²⁺- and Mn²⁺-dependences of the inhibition of EP formation by BeF_x and AlF_x. The E1Ca₂-state ATPase in 100 μM Ca²⁺ was incubated with BeF_x, AlF_x, or F⁻ alone in the presence of various concentrations of MgCl₂ or MnCl₂, and then phosphorylated by ATP, otherwise as described in Fig. 3 for E1Ca₂·BeF_x and E1Ca₂·AlF_x. The amount of EP was plotted as the percentage of that of control (incubated without BeF_x and AlF_x). Note here that the EP formation at zero Mg²⁺ or Mn²⁺ was accomplished by CaATP produced at 100 μM Ca²⁺.



Supplemental Figure 2.

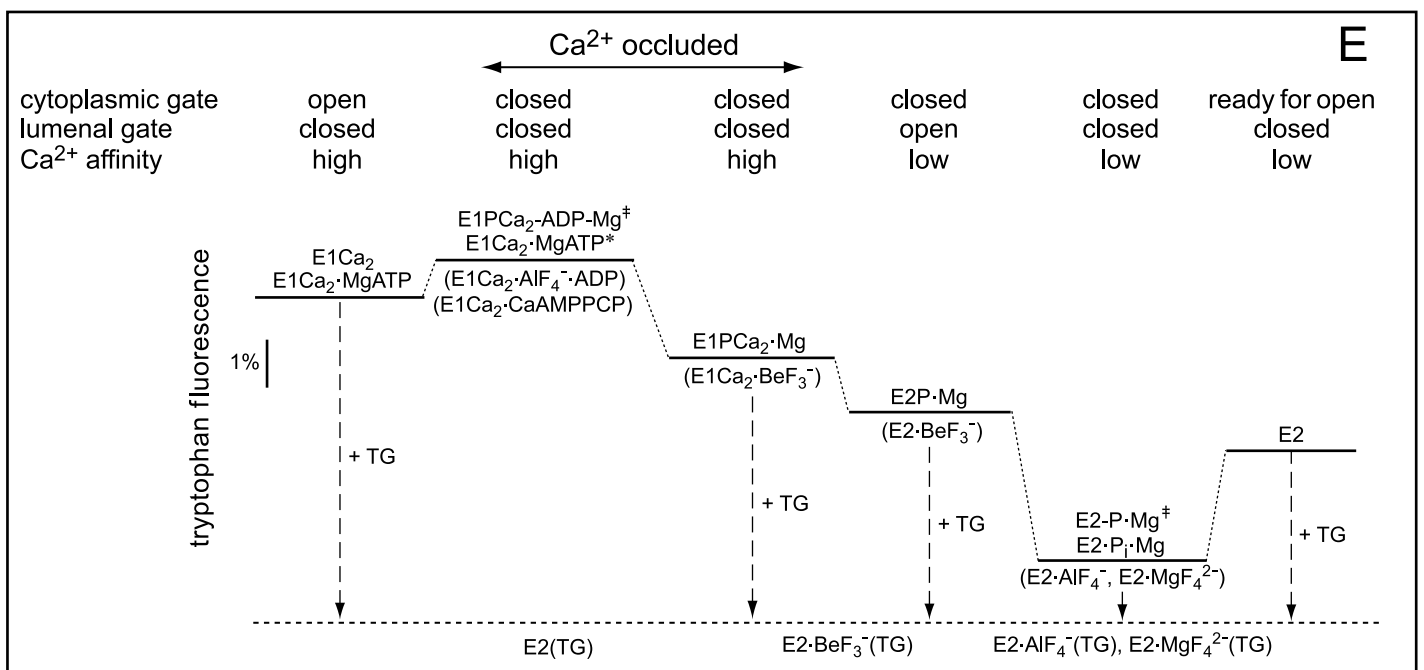
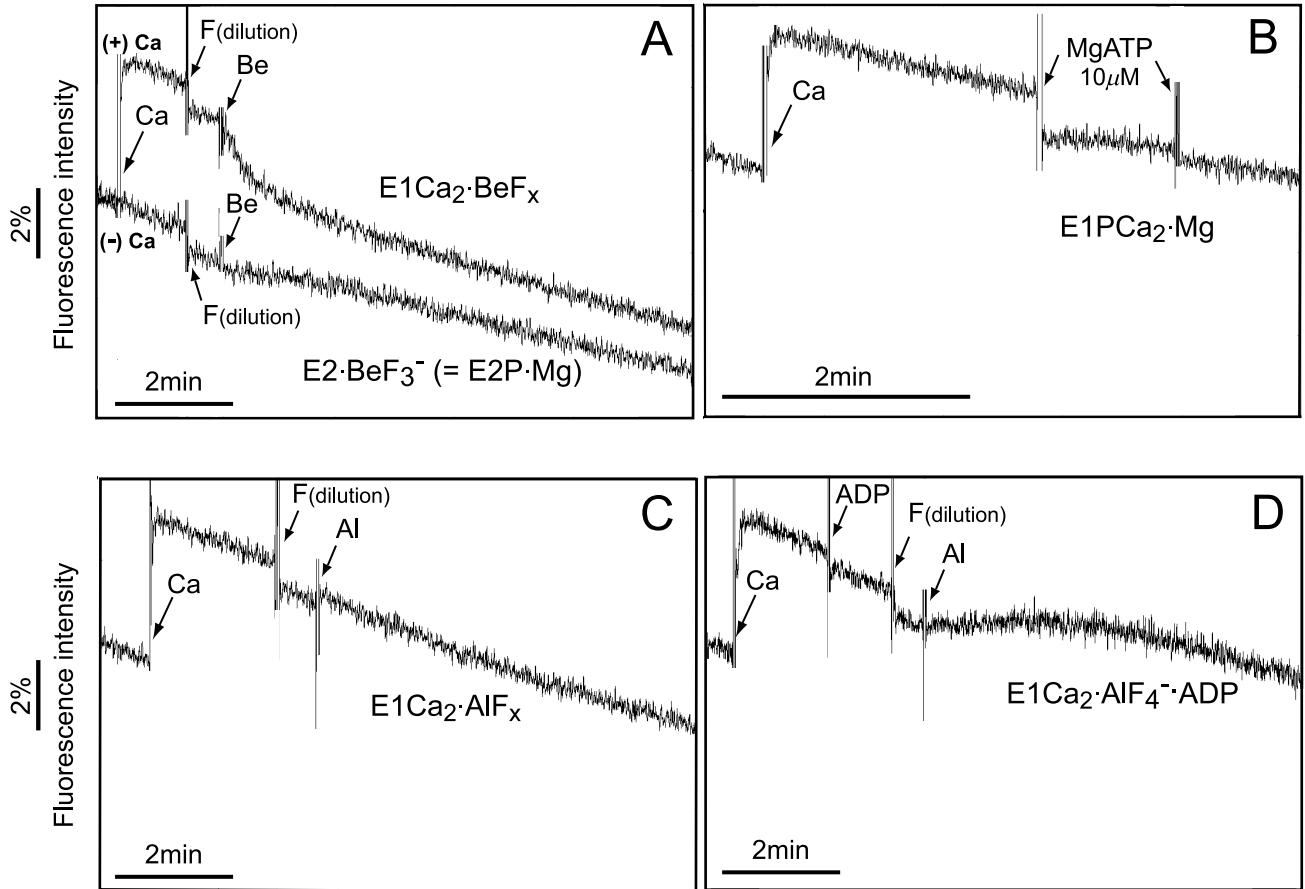
Proteolytic structural analysis of EP analogs. E1Ca₂·BeF_x, E1Ca₂·AlF_x, and E1Ca₂·AlF₄⁻·ADP were produced from the E1Ca₂ state ATPase of SR vesicles in 50 μM Ca²⁺ and 15 mM MgCl₂ at 25 °C for 10 min, and E2·BeF₃⁻ from E2 state in the absence of Ca²⁺, then subjected to the proteolysis with trypsin (*upper panel*) or proteinase K (prtK, *lower panel*). With trypsin, the 110kDa-ATPase chain is very rapidly cleaved at Arg⁵⁰⁵ (T1 site) within 0.5 min (actually completed within 10 s), producing the N- and C-terminal fragments “A” and “B”, which are not separated well (A+B) in this system. “A” was then cleaved at the T2 site (Arg¹⁹⁸), producing the C- and N-terminal fragments “A1” and “A2” (A2 is not seen because of its fast migration). With prtK, the 110kDa-ATPase chain in E1Ca₂ is rapidly cleaved at the major site Thr²⁴² on the A/M3-linker producing the fragment “p83”, whereas it becomes almost completely resistant in the ATPase complexed with the fluoride compounds. The initial rates of the production of “A1” by T2-cleavage (in the initial 1 min) and those of the 110-kDa ATPase disappearance by the prtK-Thr²⁴² cleavage (in 30 min) were obtained by the detailed time course-analyses (gels not shown for simplicity), and listed in Table 1.



Supplemental Figure 3.

Changes in tryptophan fluorescence. The measurement of tryptophan fluorescence intensity was started at 4 °C with 2.4 ml of a mixture containing SR vesicles, 15 mM MgCl₂, 0.1 M KCl, 20 mM MOPS/Tris (pH 7.0), and 0.5 mM EGTA, and then a small volume of CaCl₂ was added to give 0.6 mM or not in one trace in *A*. Subsequently, 9.6 μl of KF was added to give 2 mM, and then 2.4 μl of BeSO₄ or AlCl₃ was added to give 100 μM to produce *E1Ca₂·BeF_x* and *E2·BeF₃⁻* (*A*) or *E1Ca₂·AlF_x* (*C*). For *E1Ca₂·AlF₄⁻·ADP* formation, a small volume of ADP was added to give 50 μM before the KF addition (*D*). Note that the apparent decrease upon the F⁻ addition is due to the dilution, and F⁻ alone and F⁻ plus ADP did not change the fluorescence. (*B*) the change upon *E1PCa₂·Mg* formation by the addition of a small volume of ATP at saturating 10 μM. The extents of the changes are listed in Table 1 as the percentages of the *E1Ca₂*-state intensity. Listed also in Table 1 are the extents of the changes by the saturating 1 μM thapsigargin (TG) with the correction of the TG-induced quenching, and the extents of the changes upon formation of *E1Ca₂·MgAMPPCP* (by saturating 100 μM AMPPCP), and *E1Ca₂·CaAMPPCP* and *E1PCa₂·Ca* (by saturating 100 μM AMPPCP and 10 μM ATP, respectively, in 5 mM CaCl₂ without MgCl₂ otherwise as above). The quenching due to the absorption of excitation light by the high concentration of AMPPCP was corrected. (*E*) a schematic diagram of the tryptophan fluorescence changes thus determined at 4 °C and pH 7 for the whole Ca²⁺ transport cycle. Note, the fluorescence level of *E2·AlF₄⁻* and *E2·MgF₄²⁻* is very low and close to the *E2(TG)* level because in these states, the luminal gate is closed in contrast to the lumenally opened one in *E2·BeF₃⁻* (25). The *E2*-level varies depending on pH as in equilibrium with *E1*. *E1Ca₂·CaAMPPCP* (64) likely reflects the activated state *E1Ca₂·MgATP** (prerequisite state for phosphorylation reaction) formed by the conformational change from *E1Ca₂·MgATP* (54).

Supplemental Figure 3



Supplemental Figure 4.

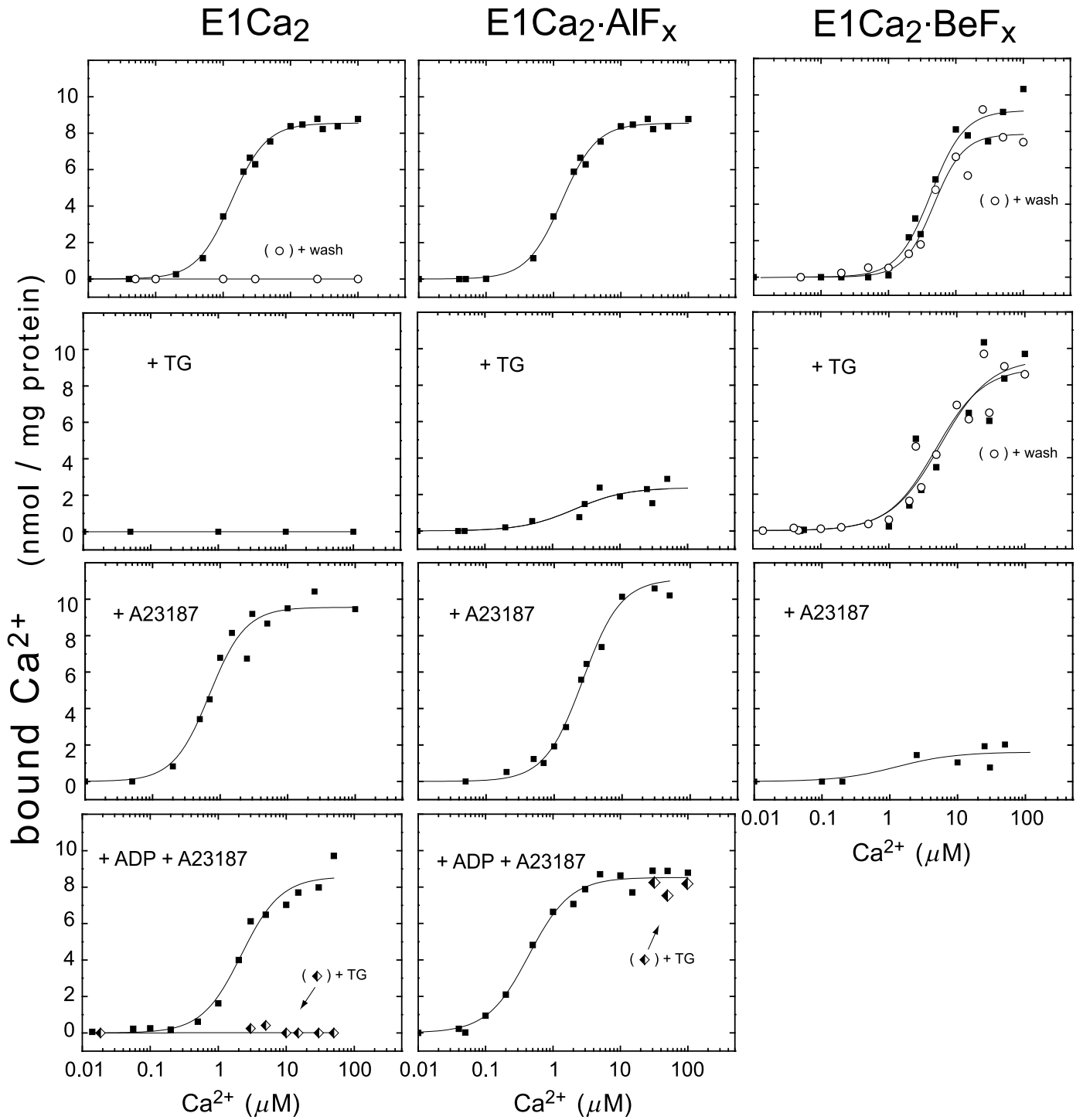
Effects of Thapsigargin and A23187 on Ca^{2+} binding in $E1\text{Ca}_2$ analogs. SR vesicles in 15 mM Mg^{2+} and various concentrations of $^{45}\text{Ca}^{2+}$ were incubated for 30 min at 25 °C with BeF_x or AlF_x to produce $E1\text{Ca}_2\cdot\text{BeF}_x$ or $E1\text{Ca}_2\cdot\text{AlF}_x$, as in Fig. 4. Then, thapsigargin (TG) at 10 μM or A23187 at 5 μM was added (*second* and *third* rows). In the *center bottom panel* ($E1\text{Ca}_2\cdot\text{AlF}_x$, +ADP+A23187), the vesicles were incubated with AlF_x and ADP to produce $E1\text{Ca}_2\cdot\text{AlF}_4\cdot\text{ADP}$ in A23187, then TG was added. At 10 min after the TG addition or at 3 s after the A23187 addition, the amount of bound $^{45}\text{Ca}^{2+}$ was determined without (*closed and half-closed symbols*) or with (*open circles*, +wash) the EGTA-washing of the membrane filter. As a control in the *top row*, the measurements were made without TG and A23187 as in Fig. 4. The amount of the background nonspecific $^{45}\text{Ca}^{2+}$ binding was determined in the presence of TG and absence of the fluoride compounds at each Ca^{2+} concentration, and subtracted.

Thapsigargin-induced Ca^{2+} Release from $E1\text{Ca}_2\cdot\text{BeF}_x$ into Lumen — The bound two Ca^{2+} in $E1\text{Ca}_2\cdot\text{BeF}_x$ were apparently not removed by TG, even with the EGTA-washing. Structural analysis with the TNP-AMP superfluorescence (Supplemental Figure 5A, B) and the proteolysis and tryptophan fluorescence (Table 1) clearly showed that $E1\text{Ca}_2\cdot\text{BeF}_x$ was rapidly converted to $E2\cdot\text{BeF}_3^-$ with bound TG. The two Ca^{2+} in $E1\text{Ca}_2\cdot\text{BeF}_x$ are therefore most probably released into and trapped in the vesicle lumen upon the TG-induced transmembrane structural perturbation and conversion to $E2\cdot\text{BeF}_3^-$. In agreement, TG is known to suppress the Ca^{2+} leakage from the lumen to cytoplasmic side because TG fixes the luminal gate in the closed state (16, 25, 55). Actually Ca^{2+} remained after the TG addition was completely lost by a calcium ionophore A23187 (data not shown).

By contrast, the occluded two Ca^{2+} in $E1\text{Ca}_2\cdot\text{AlF}_4\cdot\text{ADP}$ were not removed by TG in the presence of A23187 even with the extensive EGTA-washing. The $E1\text{Ca}_2\cdot\text{AlF}_4\cdot\text{ADP}$ resistance against TG was also revealed by the tryptophan fluorescence and proteolysis (data not shown). In $E1\text{Ca}_2\cdot\text{AlF}_x$ without ADP, the TG-induced Ca^{2+} loss and its conversion to $E2\cdot\text{AlF}_4^-$ occurred slowly (proteolysis data not shown). Thus, $E1\text{Ca}_2\cdot\text{AlF}_x$ is resistant against TG to some extent but not as strongly as $E1\text{Ca}_2\cdot\text{AlF}_4\cdot\text{ADP}$. Notably, the Ca^{2+} bound in $E1\text{Ca}_2\cdot\text{AlF}_x$ are probably released to the cytoplasmic side by TG, because the Ca^{2+} ions, if released into lumen, would be trapped in the vesicles. Therefore in $E1\text{Ca}_2\cdot\text{AlF}_x$, the cytoplasmic Ca^{2+} gate is more easily opened as compared with the luminal gate, in contrast to $E1\text{Ca}_2\cdot\text{BeF}_x$ that is prepared for the Ca^{2+} release into lumen.

Transmembrane Structural Perturbation of $E1\text{Ca}_2\cdot\text{BeF}_x$ by A23187 Causes Its Rapid Conversion to $E2\cdot\text{BeF}_3^-$ — The occluded two Ca^{2+} in $E1\text{Ca}_2\cdot\text{BeF}_x$ were rapidly lost by A23187 (Supplemental Figure 4, *third row*). The structural analyses with the TNP-AMP superfluorescence (Supplemental Figure 5C-F) and proteolysis (Table 1) demonstrated that $E1\text{Ca}_2\cdot\text{BeF}_x$ was rapidly converted to $E2\cdot\text{BeF}_3^-$ by A23187, whereas $E1\text{Ca}_2\cdot\text{AlF}_x$ and $E1\text{Ca}_2\cdot\text{AlF}_4\cdot\text{ADP}$ are resistant to A23187. Lasalocid and C_{12}E_8 at a non-solubilizing low concentration also converted $E1\text{Ca}_2\cdot\text{BeF}_x$ to $E2\cdot\text{BeF}_3^-$ as rapidly as A23187 (data not shown). As a possible cause for the conversion, some Ca^{2+} influx into or Ca^{2+} removal from the vesicle lumen is very unlikely because we observed that the A23187-induced rapid conversion $E1\text{Ca}_2\cdot\text{BeF}_x \rightarrow E2\cdot\text{BeF}_3^-$ occurs even in the presence of 0.1 mM Ca^{2+} both in the cytoplasmic and luminal sides. On the other hand, these reagents probably perturbed the transmembrane structure by the direct hydrophobic interactions, causing the rapid Ca^{2+} -deocclusion/release and the conversion to $E2\cdot\text{BeF}_3^-$. In fact, the direct interactions of the transmembrane domain with A23187 and lasalocid were demonstrated previously by the marked quenching of the tryptophan fluorescence by these reagents (28, 51, 52) due to the molecular contact with the fluorophore (57). C_{12}E_8 will surely interact with transmembrane region due to its chemical nature. The results show that $E1\text{Ca}_2\cdot\text{BeF}_x$ possesses the delicate structure ready for the isomerization to $E2\cdot\text{BeF}_3^-$ with Ca^{2+} -deocclusion/release, in contrast to $E1\text{Ca}_2\cdot\text{AlF}_4\cdot\text{ADP}$ and $E1\text{Ca}_2\cdot\text{AlF}_x$.

Supplemental Figure 4



Supplemental Figure 5.

Thapsigargin- and A23187-induced rapid conversion $E1Ca_2 \cdot BeF_x \rightarrow E2 \cdot BeF_3^-$ as revealed by TNP-AMP superfluorescence.

(A, B); $E1Ca_2 \cdot BeF_x$ (A) and $E2 \cdot BeF_3^-$ (B) were produced in 15 mM Mg^{2+} with and without 50 μM Ca^{2+} as in Fig. 5. Subsequently, TG was added to give 1 μM and the samples were incubated for 3 min, then subjected to the superfluorescence measurement with 4 μM TNP-AMP at 25 °C as in Fig. 5. Note that TG converted the $E1Ca_2 \cdot BeF_x$ -characteristic transient superfluorescence to the stable superfluorescence of $E2 \cdot BeF_3^-$ with bound TG (of which superfluorescence was reduced by 35%).

(C, D); $E1Ca_2 \cdot BeF_x$ (C) and $E2 \cdot BeF_3^-$ (D) were first produced as above, then A23187 (A23) and TNP-AMP were added successively to give 1.2 and 4 μM , respectively at 25 °C. In one trace in C and in D, A23187 was added when the maximum superfluorescence developed. Note that the A23187 addition to $E1Ca_2 \cdot BeF_x$ converted immediately the $E1Ca_2 \cdot BeF_x$ -characteristic transient superfluorescence to the stable one characteristic of $E2 \cdot BeF_3^-$. In agreement, the occluded two Ca^{2+} in $E1Ca_2 \cdot BeF_x$ were rapidly lost by A23187 even without the EGTA-washing (Supplemental Figure 4), and A23187 converted the structure from $E1Ca_2 \cdot BeF_x$ to $E2 \cdot BeF_3^-$ (proteolysis in Table 1).

(E); $E1Ca_2$ and $E2$ were first incubated with A23187, then BeF_x and TNP-AMP were added successively, otherwise as in C and D. Note that the BeF_x addition to $E1Ca_2$ in A23187 produced $E2 \cdot BeF_3^-$ but not $E1Ca_2 \cdot BeF_x$ even in 50 μM Ca^{2+} . Consistently, it was previously noted in the absence of Ca^{2+} (56) that A23187 markedly favors and accelerates the $E2 \cdot BeF_3^-$ formation from $E2$.

(F); Then we examined whether the A23187-induced rapid conversion of $E1Ca_2 \cdot BeF_x$ to $E2 \cdot BeF_3^-$ in C occurred directly ($E1Ca_2 \cdot BeF_x \rightarrow E2 \cdot BeF_3^-$) or *via* its decomposition to $E1Ca_2$ ($E1Ca_2 \cdot BeF_x \rightarrow E1Ca_2 + BeF_x \rightarrow E2 + BeF_x \rightarrow E2 \cdot BeF_3^-$). In F, we mimicked the latter reaction sequence; namely $E1Ca_2$ and $E2$ were first incubated with TNP-AMP and A23187, then BeF_x was added. The $E2 \cdot BeF_3^-$ formation from $E2$ and from $E1Ca_2$ was markedly retarded, thus the TNP-AMP binding to $E2$ and $E1Ca_2$ prior to the BeF_x addition abolished the A23187-acceleration of the $E2 \cdot BeF_3^-$ formation (*cf.* E). These results showed that the A23187-induced rapid conversion of $E1Ca_2 \cdot BeF_x$ to $E2 \cdot BeF_3^-$ in C occurs directly as $E1Ca_2 \cdot BeF_x \rightarrow E2 \cdot BeF_3^- + 2Ca^{2+}$, but not *via* its decomposition to $E1Ca_2$ and a subsequent $E2 \cdot BeF_3^-$ formation from $E2$.

Supplemental Figure 5

